Regular Article

blood

IMMUNOBIOLOGY

Therapeutic effect of JAK1/2 blockade on the manifestations of hemophagocytic lymphohistiocytosis in mice

Sophia Maschalidi,[1,2] Fernando E. Sepulveda,[1,2] Alexandrine Garrigue,[1,2] Alain Fischer,[1-4] and Geneviève de Saint Basile[1,2,5]

[1]INSERM UMR1163, Laboratory of Normal and Pathological Homeostasis of the Immune System, Paris, France; [2]Paris Descartes University-Sorbonne Paris Cité, Imagine Institute, Paris, France; [3]Immunology and Pediatric Hematology Department, Necker Children's Hospital, Assistance Publique–Hôpitaux de Paris, Paris, France; [4]Collège de France, Paris, France; and [5]Centre d'Etudes des Déficits Immunitaires, Assistance Publique–Hôpitaux de Paris, Hôpital Necker, Paris, France

Key Points

- Treatment with clinical dose of JAK1/2 inhibitor (ruxolitinib) countered manifestations of HLH in 2 cytotoxicity-impaired murine models.
- JAK1/2 inhibitor therapy in mice is effective on survival, cytopenia, inflammatory syndrome, central nervous system involvement, and liver tissue repair.

Hemophagocytic lymphohistiocytosis (HLH) is a life-threatening syndrome, characterized by severe hyperinflammation and immunopathological manifestations in several tissues. These features result from organ infiltration by overactivated CD8 T-cells and macrophages, which produce high levels of pro-inflammatory cytokines, such as IFN-γ, TNF-α, IL-6, and IL-18. Recently, several Janus kinase 1/2 (JAK1/2) inhibitors, such as ruxolitinib, have been developed as immunosuppressive agents. They have proven beneficial effects in the treatment of myeloproliferative disorders and inflammatory conditions. To determine whether pharmacological inhibition of the JAK1/2 not only prevents the onset of HLH immunopathology but also is effective against existing HLH, cytotoxicity-impaired *Prf1*$^{-/-}$ and *Rab27a*$^{-/-}$ mice with full-blown HLH syndrome were treated with a clinically relevant dose of ruxolitinib. In vivo, ruxolitinib treatment suppressed signal transducer and activator of transcription 1 activation and led to recovery from HLH manifestations in both murine models. In the *Prf1*$^{-/-}$ mice, these beneficial effects were evidenced by a greater survival rate, and in both murine models, they were evidenced by the correction of blood cytopenia and a rapid decrease in serum IL-6 and TNF-α levels. During ruxolitinib treatment, liver tissue damage receded concomitantly with a decrease in the number of infiltrating inflammatory macrophages and an increase in the number of alternatively activated macrophages. In *Rab27a*$^{-/-}$ mice, central nervous system involvement was significantly reduced by ruxolitinib therapy. Our findings demonstrate that clinically relevant doses of the JAK1/2 inhibitor ruxolitinib suppresses the harmful consequences of macrophage overactivation characterizing HLH in 2 murine models. The results could be readily translated into the clinic for the treatment of primary, and perhaps even secondary, forms of HLH. (*Blood*. 2016; 128(1):60-71)

Introduction

Hemophagocytic lymphohistiocytosis (HLH) is a rare, life-threatening syndrome, characterized by severe hyperinflammation and immunopathological manifestations in several tissues. These features result from organ infiltration by overactivated CD8 T-cells and macrophages, which produce high levels of pro-inflammatory cytokines such as IFN-γ, TNF-α, IL-6, and IL-18.[1-3] As a consequence, HLH syndrome manifests as prolonged high fever, hepatosplenomegaly, cytopenia, liver failure, and in many cases, central nervous system (CNS) manifestations. HLH can occur in many different etiological contexts. Genetic (primary) forms of HLH are a result of defects in genes involved in cytotoxic granules exocytosis or function in lymphocytes; notably, *PRF1*, *UNC13D*, *STXBP2*, *STX11*, *RAB27A*, *LYST*, and *SH2D1A*.[4-15] The failure of cytotoxic cells to kill and eliminate the infected cells and antigen-presenting cells leads to ongoing immune activation and the canonical features of HLH.[16-18] Although the genetic forms of HLH primarily affect infants and children, the number of confirmed cases in adolescents and adults is growing.[4,5,19,20] Secondary forms of HLH are caused by a variety of underlying conditions and are more frequent than the primary forms. They occur in the context of severe viral infections, especially Epstein-Barr virus infection, cancer, and autoinflammatory and autoimmune diseases, in all age groups.[3,21,22] The probably diverse mechanisms that lead to secondary HLH are largely unknown.

If not treated, primary HLH is generally fatal. Delayed treatment initiation increases the risk for neurological complications.[23-26] The initial therapy consists of chemotherapeutic agents (ie, etoposide) or immunosuppressive agents (eg, antithymoglobulin) combined with steroids and cyclosporine A. The goal is to suppress the hyperinflammatory component of the disease and eliminate activated cytotoxic lymphocytes and macrophages.[27,28] Treatment of CNS involvement may require intrathecal chemotherapy.[29] In a second step, allogenic hematopoietic stem cell transplantation (HSCT) is required

Submitted February 15, 2016; accepted May 10, 2016. Prepublished online as *Blood* First Edition paper, May 24, 2016; DOI 10.1182/blood-2016-02-700013.

The online version of this article contains a data supplement.

The publication costs of this article were defrayed in part by page charge payment. Therefore, and solely to indicate this fact, this article is hereby marked "advertisement" in accordance with 18 USC section 1734.

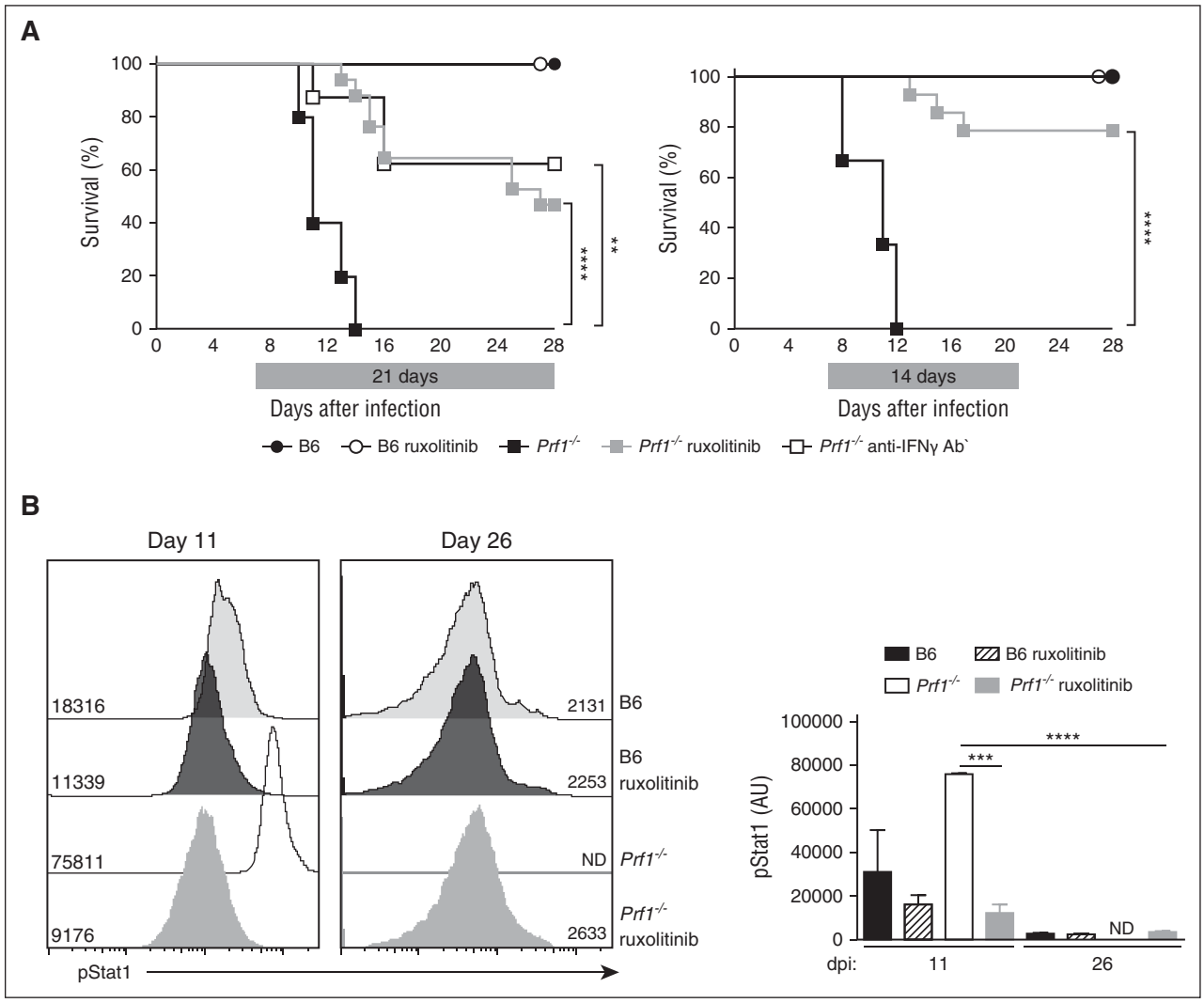

Figure 1. Ruxolitinib therapy improves the survival of infected *Prf1*$^{-/-}$ mice and suppresses STAT1 activation in vivo. (A) Control (B6) and perforin-deficient (*Prf1*$^{-/-}$) mice infected with LCMV on day 0 were treated with either JAK1/2 inhibitor (ruxolitinib) or vehicle solution alone from day 7 to day 28 (21 days treatment; left) or from day 7 to day 21 (14 days treatment; right). A group of *Prf1*$^{-/-}$ mice was treated with anti-IFNγ antibody given every third day from day 7 until day 16. Data (mean ± SEM) are representative of 3 to 4 independent experiments with at least 3 mice in each group. $^{**}P < .005$; $^{****}P < .0001$. Survival was analyzed with a log-rank test (Mantel-Cox) (n = 5-17). (B, left) Representative fluorescence-activated cell sorter analysis of pStat1 levels in the blood MNCs from control (B6) and *Prf1*$^{-/-}$ mice treated with ruxolitinib or not and analyzed at 2 different times. (Right) Quantification of mean fluorescence intensity of pStat1 in the blood MNCs from control and *Prf1*$^{-/-}$ mice treated with ruxolitinib or not at the day postinfection indicated. At each point, measurement was performed 1 hour after gavage with ruxolitinib. ND, not determined for nontreated *Prf1*$^{-/-}$ mice that do not survive. Data (mean ± SD) represent 3 to 4 mice in each group. $^{***}P < .001$; $^{****}P < .0001$.

to prevent recurrences of HLH in the genetic forms of the disease.[27,28,30,31] With the current standard of care, approximately 20% to 25% of HLH sufferers die before HSCT, mostly as a result of inadequate disease control or serious complications of immunosuppressive or chemotherapeutic treatments.[26,28,30,32] Hence, there is an urgent unmet medical need for developing less toxic, more effective, and more targeted immunosuppressive treatments in HLH.

Several HLH-promoting cytokines have been identified, and are therefore candidate targets for reducing hyperinflammation. They include IFN-γ, IL-2, TNF-α, IL-6, and IL-18.[1-3,33] IFN-γ appears to have a particularly critical role. Serum IFN-γ levels and interferon signature are generally found to be elevated during the initial course of HLH, and the cytokine is produced by lymphocytes infiltrating the liver of patients with HLH, regardless of the HLH's underlying cause.[33-37] Targeting IFN-γ also appears to be a particularly promising approach when considering the results of studies in cytotoxicity-impaired murine models of HLH, in which the condition is triggered by infection with lymphocytic choriomeningitis virus (LCMV). In fact, IFN-γ is pivotal for macrophage activation in these murine models, as neutralization of the cytokine with specific antibody significantly reduces macrophage activation.[38,39] A phase 2 clinical trial of an anti-IFN-γ monoclonal antibody is underway.[40]

Janus kinase (JAK) inhibitors are now in clinical development as anti-inflammatory and immunosuppressive agents. JAK1/2 inhibitors, such as ruxolitinib, a compound already approved by the US Food and Drug Administration (FDA) for the treatment of intermediate or high-risk myelofibrosis, have demonstrated clinical efficacy in rheumatoid arthritis, myeloproliferative disorders, psoriasis, and alopecia areata.[41-45] JAK1 and JAK2 control the signaling of many cytokines; notably, IFN-γ, IL-2, and IL-6. On binding to a cytokine receptor, JAKs transactivate and phosphorylate the latter's cytoplasmic domain, which leads to the recruitment and phosphorylation of signal transducer and activator of transcription (STAT). The STAT then dimerizes, translocates to the nucleus, and activates gene transcription.[46] Furthermore, JAK/STAT

signaling in macrophages can be indirectly activated by innate immune receptors, such as TLRs and TNF receptors, which confer JAK inhibitor with a broad spectrum of activity.[47]

In view of the efficacy of the JAK1/2 inhibitor ruxolitinib in other inflammatory conditions and its ability to block the signaling of several key inflammatory cytokines that are overproduced during the course of HLH, JAK1/2 inhibition might represent a promising therapeutic approach for HLH. Of note, prevention of the development of HLH manifestations by administration of high-dose ruxolitinib has been recently reported in the murine model of primary (*Prf1*$^{-/-}$) and secondary (CpG-induced) HLH.[48] To determine whether or not the drug also has therapeutic efficacy on the HLH manifestations and survival, we treated 2 cytotoxicity-impaired murine models, the *Prf1*$^{-/-}$ and the *Rab27a*$^{-/-}$ mice, at the time they expressed the full-blown syndrome. We found that a short period of treatment with a clinically relevant dose of ruxolitinib significantly increased long-term survival, relative to nontreated mice; corrected most of the harmful clinical, biological, and histological features of HLH, including CNS cell infiltration; and promoted liver tissue repair.

Methods

Mice and mice studies

C57BL/6J wt, C57BL/6J-Prf1^{tm1Sdz}/J (*Prf1*$^{-/-}$), and C57BL/6J- Rab27a^{ash}/J (*Rab27a*$^{-/-}$) have been described previously.[39] Mice were treated or not with ruxolitinib (1 mg/kg) twice daily by oral gavage starting at day 7 in *Prf1*$^{-/-}$ and at day 10 in *Rab27a*$^{-/-}$ postinfection. Ruxolitinib was prepared from 5-mg commercial tablets in PEG300/dextrose 5% dissolved in a ratio of 1:3, as previously reported.[49] Anti-INF-γ (XMG1.2) treatment consisted of 4 intraperitoneal injections of 1 mg antibody/mouse given every third day, from day 7 until day 16. Induction of HLH by LCMV infection and analysis of the clinical, biological, and histological parameters of HLH, as well as determination of viral titers in mice, were performed as previously described[17,50] and as detailed in the supplemental Methods, available on the *Blood* Web site.

Cell isolation, sorting of macrophages, and flow cytometry analysis

Isolation of liver mononuclear cells (MNCs) was performed as previously described[51] and is detailed in supplemental *Methods*. For sorting of macrophages, cells were gated on CD45.2$^+$ F4/80$^+$ macrophages and then sorted as F4/80^{high}CD11b^{low}LY6C^{low} for Kupffer cells, F4/80$^+$CD11b$^+$LY6C^{high} for inflammatory macrophages, and F4/80$^+$CD11b$^+$LY6C^{low} for alternatively activated macrophages.

For detection of intracellular markers (phosphorylated Stat1 [pStat1] and pStat5), RAW 264.7 cells or blood from mice during LCMV infection time-course were fixed and permeabilized with the BD Phosflow kit and then stained with anti-Stat1 (pY701) and anti-Stat5 (pY701) antibodies.

Statistical analysis

Data were analyzed with GraphPad Prism 6 software. Survival and HLH incidence curves were analyzed by using the log-rank (mantel-Cox) test. All other analyses were performed by using *t* tests or one-way ANOVA with posttest. Differences were considered to be statistically significant when $P < .05$ (indicated as $*P < .05$, $**P < .01$, $***P < .001$, $****P < .0001$).

Results

Therapeutic use of the JAK1-2 inhibitor ruxolitinib improves the survival of *Prf1*$^{-/-}$ mice

We used perforin-deficient (*Prf1*$^{-/-}$) mice to determine the potential therapeutic benefits of JAK inhibition in an HLH setting, as these animals develop a very severe disease that closely mimics human HLH. To this end, control (B6) mice and *Prf1*$^{-/-}$ mice were infected with LCMV (200 PFU) and treated orally with the FDA-approved JAK1/2 inhibitor ruxolitinib (1 mg twice daily) or vehicle alone for 21 days. Treatment started from day 7 after LCMV infection once the mice presented with full-blown HLH syndrome (Figure 1A). As expected, all the *Prf1*$^{-/-}$ mice that had received vehicle succumbed to the infection between days 8 and 14 postinfection, whereas all the control B6 mice survived (Figure 1A). Ruxolitinib treatment was associated with significantly greater survival of *Prf1*$^{-/-}$ mice, relative to vehicle-treated *Prf1*$^{-/-}$ mice, as 50% of the animals were alive at day 28 postinfection. Treatment with an anti-IFN-γ antibody, previously shown to significantly improve survival and HLH features in *Prf1*$^{-/-}$ mice, was tested in the same experiment for comparative purposes. When initiated on day 7 and given every 3 days for the next 12 days, treatment with anti-IFN-γ antibody yielded much the same survival rate among the *Prf1*$^{-/-}$ mice as ruxolitinib did (Figure 1A). We noted that the deaths of *Prf1*$^{-/-}$ mice treated for 21 days with ruxolitinib occurred in 2 phases: an early phase, probably resulting from HLH disease, in most animals and a late phase (> day 24) in a few animals. We hypothesize that late-phase mortality might be a result of an adverse drug reaction associated with drug administration in fragile *Prf1*$^{-/-}$ mice. We therefore tested a shorter treatment period (14 days) and found that it was associated with a remarkably higher survival rate in *Prf1*$^{-/-}$ mice, as no deaths occurred after treatment cessation (Figure 1A). The 14-day protocol was therefore used in subsequent experiments.

Ruxolitinib's in vivo efficacy was also evaluated by measuring levels of pSTAT1 in white blood cells sampled from treated and nontreated LCMV-infected *Prf1*$^{-/-}$ mice. A significant and gradual decrease over time in pSTAT1 levels was detected in blood leukocytes sampled from ruxolitinib-treated *Prf1*$^{-/-}$ mice, analyzed 1 hour after gavage, between day 11 and day 26 postinfection (Figure 1B). Similarly, a progressive decrease over time in pSTAT1 and pSTAT5 levels was detected in vitro when RAW264.7 macrophages were stimulated with recombinant IFN-γ in the presence of an increased concentration of ruxolitinib (supplemental Figure 1A). A wide range of IFN-γ-responsive genes is expressed after STAT's phosphorylation and translocation to the nucleus, including inducible expressed GTPase, class II major histocompatibility complex transactivator, and C-X-C motif chemokine 10 (CXCL10), also known as interferon γ-induced protein 10. IFN- γ responsive expression of all 3 genes was dramatically downregulated in IFN-γ-activated RAW264.7 macrophages preincubated with ruxolitinib (supplemental Figure 1B).

Improvement of clinical and biological manifestations of HLH during ruxolitinib therapy

We compared the features of HLH in nontreated and ruxolitinib-treated *Prf1*$^{-/-}$ mice. After LCMV infection, nontreated *Prf1*$^{-/-}$ mice lost body weight and developed hypothermia, lethargy, hunched posture, and shaking before death. Mice receiving the ruxolitinib JAK1/2 inhibitor progressively controlled their hypothermia and gradually regained mobility and activity when compared with nontreated *Prf1*$^{-/-}$ mice. At later times, the treated *Prf1*$^{-/-}$ mice started to regain weight and achieved a normal body temperature between days 30 and 55 (Figure 2A). In control mice, only transient decreases in body weight, body temperature, and physical activity were observed, regardless of whether or not ruxolitinib was administered (Figure 2A).

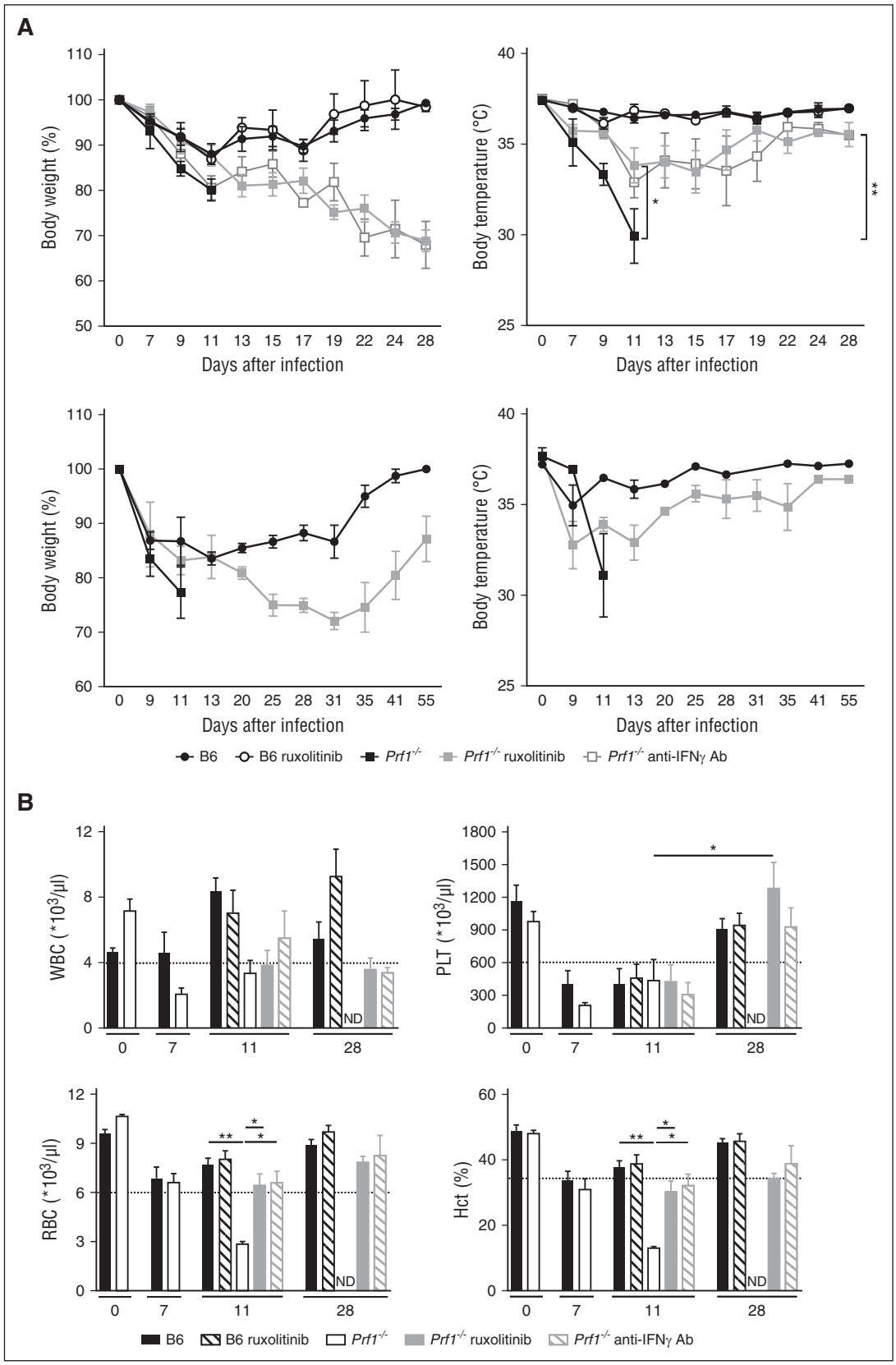

Figure 2. Ruxolitinib therapy improves clinical and hematological parameters of HLH in *Prf1*$^{-/-}$ mice. (A) Body weight (left) and body temperature (right) of B6 and *Prf1*$^{-/-}$ mice infected at day 0 and receiving ruxolitinib treatment or not during 14 days, or anti- IFN-γ antibody every third day, from day 7 until day 16, and then followed up to day 28 (upper) or receiving ruxolitinib treatment during 21 days and followed up to day 55 (lower). *$P < .05$; **$P < .005$. (B) Hematological parameters (white blood cells [WBC], platelets [PLT], red blood cells [RBCs], and hematocrit [Hct]) at different times (days 0-28 postinfection) of nontreated control (B6) mice and *Prf1*$^{-/-}$ mice nontreated, treated with ruxolitinib from day 7 postinfection for 14 days, or treated with anti-IFN-γ antibody from day 7 until day 16. Dotted lines represent normal values. Data (mean ± SEM) are representative of 2 to 4 independent experiments with at least 3 mice in each group. *$P < .05$; **$P < .005$.

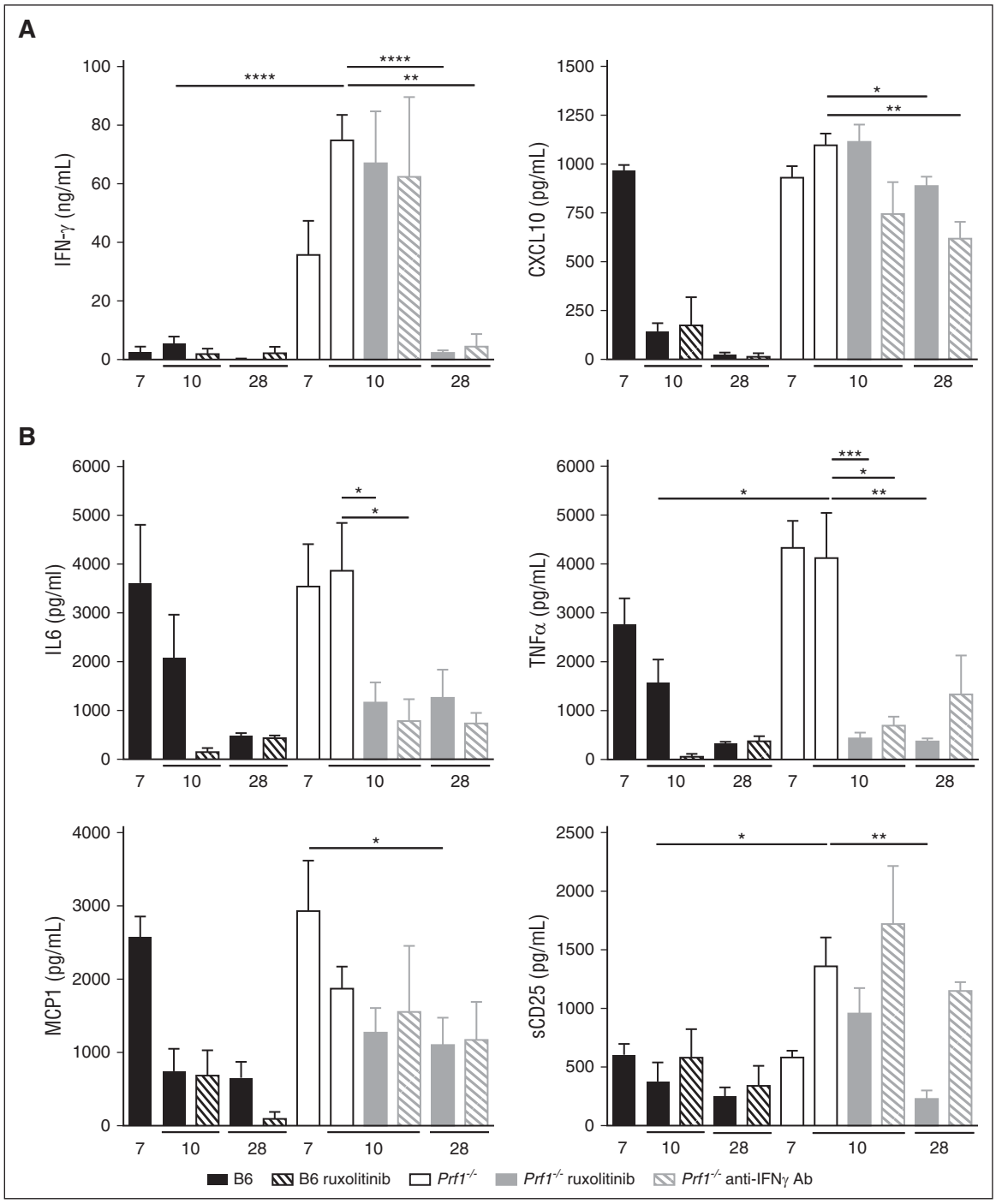

Figure 3. Ruxolitinib therapy decreases serum levels of inflammatory cytokines and chemokines in infected *Prf1*$^{-/-}$ mice. Serum levels of IFN-γ and CXCL10, and (B) serum levels of IL-6, TNF-α, MCP1, and sCD25 were measured at different points (on days 7, 10, and 28) in control (B6) and *Prf1*$^{-/-}$ mice nontreated, treated with ruxolitinib from day 7 postinfection for 14 days, or treated with anti-IFN-γ antibody from day 7 until day 16. Data (mean ± SEM) are representative of 2 to 3 independent experiments with at least 3 mice in each group. *$P < .05$; **$P < .005$; ***$P < .001$; ****$P < .0001$.

Severe pancytopenia, including anemia, leucopenia, and thrombocytopenia, is also a prime feature of HLH manifestations in both patients and murine models[29,38] We found that the *Prf1*$^{-/-}$ mice had recovered from anemia and leucopenia on day 12 (5 days after treatment initiation) and had achieved a normal thrombocyte count on day 15 (Figure 2B and data not shown). All these parameters were still within the normal range at day 37 post-infection (data not shown), showing that the retrieval of treatment did not compromise the correction of pancytopenia, even for a long-lasting LCMV infection.

HLH disease manifests as a hyperinflammatory condition with elevated levels of IFN-γ and inflammatory cytokines.[33,37,38] Indeed, serum IFN-γ level was dramatically higher in *Prf1*$^{-/-}$ mice than in control mice, with a peak at day 10 after LCMV infection (Figure 3A). As expected, a similar peak was detected at day 10 in *Prf1*$^{-/-}$ mice receiving ruxolitinib, as it acts

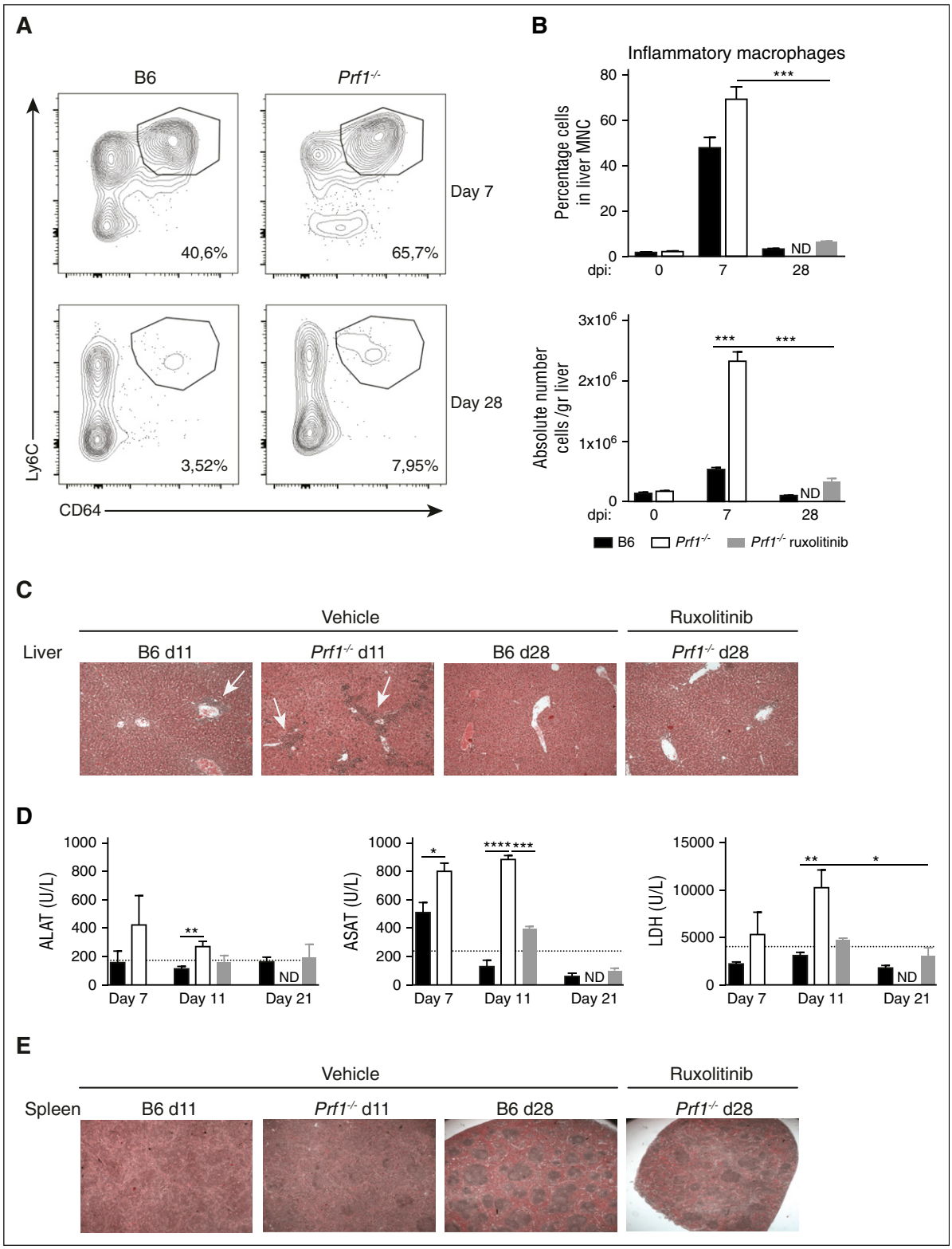

Figure 4. Ruxolitinib therapy reduces macrophage activation, tissue infiltration, and tissue damage. (A) Representative fluorescence-activated cell sorter analysis of liver MNCs gated on $CD64^+$ $Ly6C^+$ inflammatory macrophages in control (B6) and $Prf1^{-/-}$ mice nontreated (day 7) or treated with ruxolitinib for 14 days (day 28). (B) Frequency and absolute number of inflammatory $CD64^+Ly6C^+$ macrophages in the liver at the indicated point (dpi [days postinfection]; upper and lower, respectively). Data (mean ± SEM) are representative of 3 to 4 independent experiments with at least 3 mice in each group. ***$P < .001$. (C) Hematoxylin and eosin staining of liver sections from untreated control mice (B6) (days 11 and 28) and $Prf1^{-/-}$ mice either nontreated (day 11) or treated with ruxolitinib and analyzed at day 28 postinfection (10× objective lens). Periportal and parenchymal infiltrates are depicted with arrows. One representative of at least 5 randomly chosen fields is shown. (D) Aspartate aminotransferase (ASAT), alanine transaminase (ALAT), and lactate dehydrogenase (LDH) levels in the serum from (B6) and $Prf1^{-/-}$ mice either nontreated or treated with ruxolitinib from day 7 postinfection for 14 days, and measured at different points. *$P < .05$; **$P < .005$; ***$P < .001$; ****$P < .0001$). Dotted lines represent normal values. (E) Hematoxylin and eosin staining of spleen sections from control (B6) at day 11 and day 28 and $Prf1^{-/-}$ mice either nontreated (day 11) or treated with ruxolitinib and analyzed at day 28 postinfection (5× objective lens). One representative of at least 5 randomly chosen fields is shown. Data (mean ± SEM) are representative of 3 to 4 independent experiments with at least 3 mice in each group.

downstream of the IFN-γ receptor. In *Prf1*$^{-/-}$ mice, increased IFN-γ secretion was associated with elevated serum levels of CXCL10, IL-6, TNF-α, and monocyte chemoattractant protein-1 (MCP-1) (Figure 3A-B). Remarkably, serum IL-6 and TNF-α levels were dramatically lower in treated *Prf1*$^{-/-}$ mice and reached levels close to those observed in control mice 3 days after treatment initiation (Figure 3B). The high levels of MCP-1 and CXCL10 had fallen slightly but significantly at day 28 (Figure 3A). Levels of soluble IL-2 receptor (sCD25) are commonly elevated in HLH disease.[52] In fact, elevated sCD25 levels were also detected in *Prf1*$^{-/-}$ mice and fell steadily once ruxolitinib treatment had been initiated. Treatment of *Prf1*$^{-/-}$ mice with an anti-IFN-γ antibody had a similar beneficial effect on the clinical and biological HLH features in the surviving mice when analyzed in parallel (Figures 2 and 3). A similar, beneficial effect of ruxolitinib therapy on clinical and biological features and serum cytokine levels was observed in *Rab27a*$^{-/-}$ mice (supplemental Figure 2A and data not shown). Hence, ruxolitinib therapy in 2 different murine models rapidly improved the characteristic clinical and biological features and hypercytokinemia associated with HLH disease.

Reduction of tissues infiltration by inflammatory macrophages during ruxolitinib therapy

Given that macrophage activation and organ infiltration by activated MNCs are hallmarks of HLH, we analyzed the number and phenotype of macrophages in various tissues. In the liver, both *Prf1*$^{-/-}$ mice and control mice displayed an increase in the inflammatory macrophage ($CD64^+Ly6C^+$) count. The absolute number of inflammatory macrophage count was much higher in *Prf1*$^{-/-}$ mice than in control mice at 7 days postinfection (Figure 4A-B). After 2 weeks of ruxolitinib treatment, *Prf1*$^{-/-}$-treated mice and control mice had a similar number of inflammatory macrophages in the liver (Figure 4A-B). Liver sections evidenced prominent cell infiltrates in the portal tract and the parenchyma of infected *Prf1*$^{-/-}$ mice on day 11 postinfection. These cell infiltrates were also present, albeit to a lesser extent, in control mice at this point (Figure 4C). Remarkably, cell infiltrates were no longer detectable in the liver of *Prf1*$^{-/-}$ mice after 2 weeks of ruxolitinib treatment, as in nontreated control mice (Figure 4C). Serum levels of aspartate aminotransferase, alanine, and lactate dehydrogenase, markers of liver disease, were significantly higher in *Prf1*$^{-/-}$ mice than in control mice, but fell rapidly after 3 days of ruxolitinib treatment (Figure 4D). Ruxolitinib's therapeutic effects on cell infiltration of the liver and liver damage were also obvious when liver sections from treated and nontreated *Rab27a*$^{-/-}$ mice were compared at day 25 postinfection (supplemental Figure 3A).

Splenomegaly was observed in all mouse strains at day 11 postinfection, regardless of the genetic status or treatment (data not shown); this is a well-known feature of acute LCMV infection.[38] In nontreated *Prf1*$^{-/-}$ mice at day 11 postinfection, the splenic architecture was disrupted, and red and white pulp zones were completely disorganized. However, the mice's splenic architecture was fully restored by 2 weeks of ruxolitinib treatment (Figure 4E). Very similar observations were made for treated vs nontreated *Rab27a*$^{-/-}$ mice at day 25 (supplemental Figure 3B). Involvement of the CNS is 1 of the major concerns in humans HLH.[23,26] Because meningeal infiltration is not detectable at day 12 postinfection in *Prf1*$^{-/-}$ mice (ie, before mice died),[38,39] the nonfatal *Rab27a*$^{-/-}$ murine model of HLH was used to evaluate ruxolitinib's efficacy in CNS disease. As previously reported,[39] we found that *Rab27a*$^{-/-}$ mice displayed diffuse, intraparenchymal cell infiltration at day 25 after LCMV postinfection (supplemental Figure 3C). In contrast, no intraparenchymal cell infiltration was observed in ruxolitinib-treated *Rab27a*$^{-/-}$ mice studied at the same time (supplemental Figure 3C). Thus, brain tissue infiltration in cytotoxicity-impaired mice is dramatically lower in ruxolitinib-treated mice than in nontreated mice.

Taken as a whole, these results in murine models show that treatment with JAK1/2 inhibitor ruxolitinib significantly reduces the inflammatory macrophage activation and tissue infiltration that characterize HLH disease.

Improvement of tissue repair during ruxolitinib therapy

In addition to infiltration of the liver by MNCs, tissue damage in *Prf1*$^{-/-}$ mice at day 11 postinfection is characterized by intense fibrosis and collagen deposition. These features completely resolved after 2 weeks of ruxolitinib treatment (Figures 5A-C and 6A). Although control mice experienced an acute increase in cell infiltration and liver fibrosis early in the course of infection, these parameters then normalized as liver tissue repair proceeded (Figure 5A-C). However, we noticed that even after recovery of liver damage, the MNCs count in the liver of treated *Prf1*$^{-/-}$ mice was still greater than in the liver of control mice (Figure 5B). We therefore hypothesized that a restorative cell population present in or moving into the liver may participate in the recovery phase of ruxolitinib-treated *Prf1*$^{-/-}$ mice.

Hepatic macrophages, which make up a heterogeneous, plastic population with varying transcriptional and functional profiles, have a range of roles in both the induction and resolution of inflammation.[53,54] We thus investigated gene expression profiles and macrophage polarization of MNCs isolated from the liver of *Prf1*$^{-/-}$ and control mice during the course of infection and treatment. During the early phase of the HLH-disease (day 7 postinfection), we noted an increase in the transcription levels of *Ifn*γ and *Nos2,* a biomarker of macrophage inflammation[55] (Figure 5C). At day 10 post-infection, the transcription of *Nos2* fell in control mice, whereas the transcription of *Chil3*, a marker of tissue repair,[56] was upregulated (Figure 5C). In *Prf1*$^{-/-}$ mice the expression levels of all 3 transcripts were much higher than in control mice but followed the same time course (Figure 5C). However, it was noticeable that ruxolitinib treatment of the *Prf1*$^{-/-}$ mice (initiated 4 days previously) accelerated the fall in *Nos2* expression and the increase in *Chil3* expression. At later times (days 21-28), MNCs isolated from ruxolitinib-treated *Prf1*$^{-/-}$ mice displayed a high expression level of *Il10* (Figure 5C). The cytokine IL10 is well-known for its anti-inflammatory effects and regulatory effects on immune responses. The level of *Ifn*γ fell progressively, in parallel with that of *Cxcl10* in liver MNCs isolated from both control and *Prf1*$^{-/-}$-treated mice (supplemental Figure 4A).

We also monitored the distributions of tissue-resident and monocyte-derived macrophage subsets in the liver of infected mice during both the development and resolution phases of HLH disease. Three subsets of $CD45^+F4/80^+$ macrophages were analyzed, based on the presence or absence of well-established cell surface markers: the $F4/80^{high}CD11b^{low}LY6C^{low}$ subset of resident macrophages (also known as Kupffer cells), the $F4/80^+CD11b^+LY6C^{high}$ subset of inflammatory macrophages, and the $F4/80^+CD11b^+LY6C^{low}$ subset of alternatively activated macrophages, responsible for immunomodulation and wound-healing responses.[53] The 3 cell subsets had distinct morphologies (supplemental Figure 4B), as suggested previously.[57] The relative proportion and absolute count of each macrophage subset varied considerably during the course of the study. In control mice, the Kupffer cell count fell rapidly in the first 7 days postinfection and then rapidly returned to normal values at

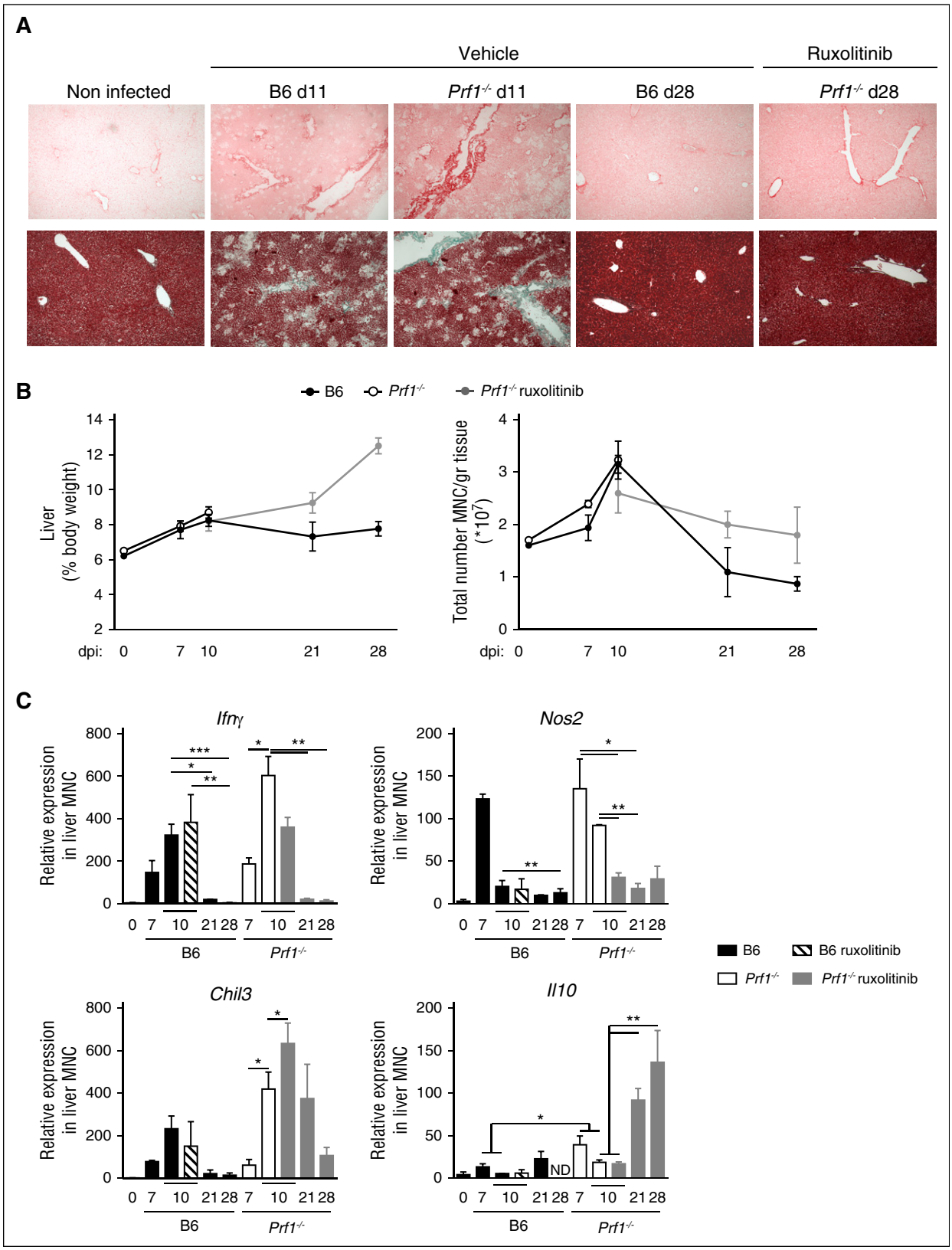

Figure 5. LCMV-induced liver damage shows distinct phases of fibrosis and resolution improved by ruxolitinib therapy. (A) Histological analysis of hepatic fibrosis using PicroSirius red staining (upper) and Masson's Trichome (lower) from nontreated control mice (B6) (days 11 and 28) and *Prf1*$^{-/-}$ mice either nontreated (day 11) or treated with ruxolitinib and analyzed at day 28 postinfection. One representative of at least 5 randomly chosen fields is shown. (B, left) Liver size and (right) absolute number of MNCs in the liver of control (B6) and *Prf1*$^{-/-}$ mice nontreated or treated for 14 days from day 7 postinfection. (C) Relative expression of *Ifnγ*, *Nos2*, *Chil3*, and *Il10* in liver MNCs obtained before or after LCMV infection in control (B6) and *Prf1*$^{-/-}$ mice either nontreated or treated with ruxolitinib. Data (mean ± SEM) are representative of 2 independent experiments with at least 3 mice in each group. **P* < .05; ***P* < .005; ****P* < .001.

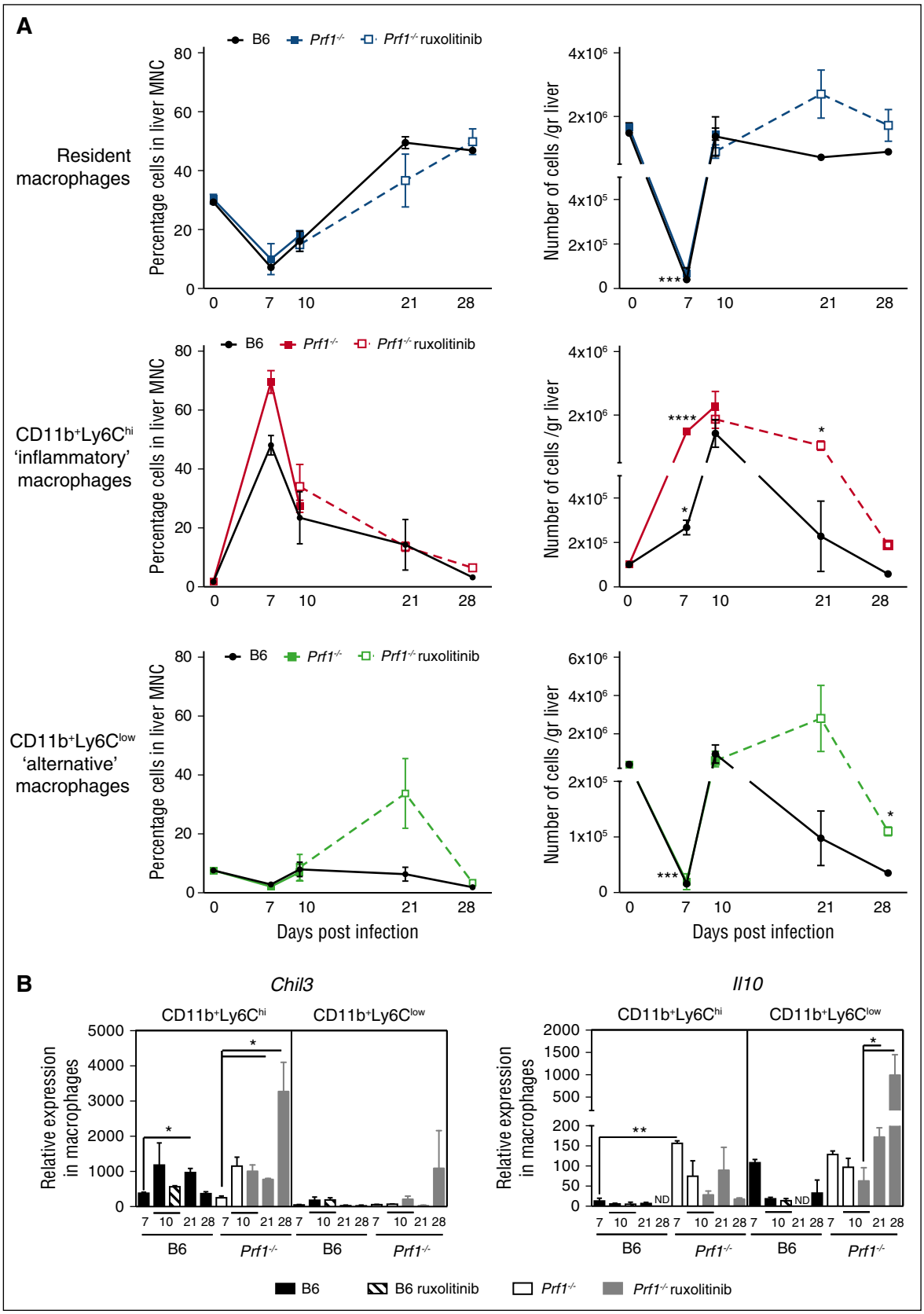

Figure 6. The early inflammatory response to LCMV is counter balanced by a pronounced restorative response in *Prf1*$^{-/-}$ mice treated with ruxolitinib. (A) Analysis of the relative (left) and absolute (right) number of each macrophage subset expressed as relative to mean total macrophage number in the liver of control (B6) and *Prf1*$^{-/-}$ mice either nontreated or treated with ruxolitinib for 14 days at the indicated times. Data (mean ± SEM) are representative of 2 independent experiments with at least 3 mice in each group. *$P < .05$; ***$P < .001$; ****$P < .0001$). (B) Relative expression of *Chil3* and *Il10* in sorted hepatic macrophages obtained after LCMV infection from control (B6) and *Prf1*$^{-/-}$ mice either nontreated or treated with ruxolitinib for 14 days, at the indicated times. Data (mean ± SEM) are representative of 2 independent experiments with at least 3 mice in each group. *$P < .05$; **$P < .005$.

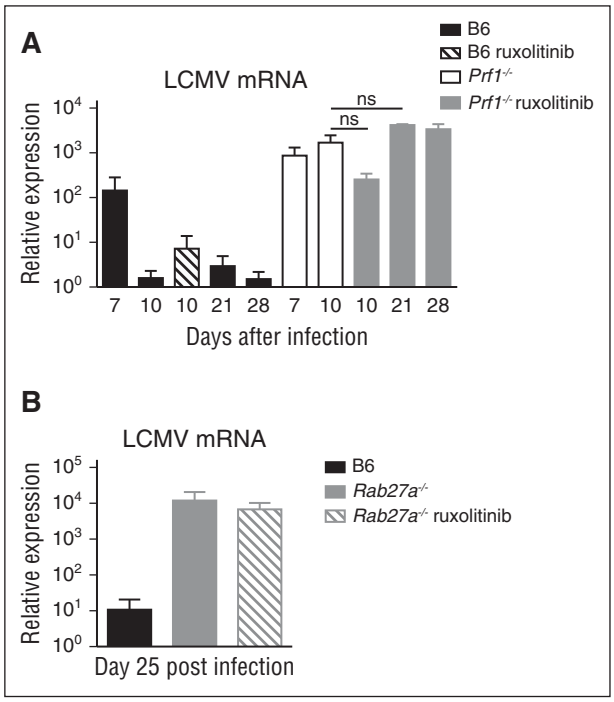

Figure 7. Ruxolitinib therapy does not influence virus load in LCMV infected cytotoxicity-deficient mice. (A) Viral titers in the liver from control (B6) and *Prf1*$^{-/-}$ mice and (B) of control (B6) and *Rab27a*$^{-/-}$ mice nontreated or treated with ruxolitinib for 14 days and analyzed at the indicated points. Data (mean ± SEM) are representative of 3 independent experiments with at least 3 mice in each group. ns, nonsignificant.

day 10 postinfection, as previously shown in other infectious settings[51] (Figure 6A). Thereafter, the concomitant infiltration of the liver by inflammatory and alternatively activated macrophage subsets vanished rapidly in control mice. A similar time course for the distribution of macrophage subsets was observed in the *Prf1*$^{-/-}$ mice during the early phase of infection (up to 10 days) (Figure 6A). However, in ruxolitinib-treated *Prf1*$^{-/-}$mice, the fall in the inflammatory macrophage count between days 10 and 28 postinfection was associated with an increase in the number of Kupffer cells and, more importantly, alternatively activated macrophages, which peaked at day 21 before returning to normal values at day 28 (Figure 6A). It should be noted that both subsets of activated macrophages can express *Chil3* and *Il10* transcripts during the liver recovery phase (Figure 6B), although *Il10* was much more strongly expressed in CD11^{+}Ly6C^{low} macrophages at later points. These findings further argue in favor of a functional switch between these macrophage subsets and highlight the limitations of the conventional phenotypic approach to functionally distinguishing between macrophage populations in vivo. Increased numbers of the latter 2 macrophage subsets in *Prf1*$^{-/-}$-treated mice probably accounted for the high level of *Chil3* and *Il10* transcripts detected in the MNCs in the liver of *Prf1*$^{-/-}$-treated mice. During ruxolitinib treatment, *Prf1*$^{-/-}$ mice were able to successfully control tissue damage through the distinct, sequential complementary actions of the 2 main macrophage populations infiltrating the liver. Because the direct benefit of ruxolitinib therapy in treated vs nontreated *Prf1*$^{-/-}$ mice in this respect could not be compared, given the rapid death of the nontreated animals, we used *Rab27a*$^{-/-}$ mice to address this issue. Interestingly, a beneficial action of ruxolitinib therapy on the time course of tissue repair, as determined by specific gene transcripts in the MNCs isolated from the liver, was apparent at day 25 postinfection (ie, 2 weeks after initiation of the treatment) in treated *Rab27a*$^{-/-}$ mice, relative to nontreated mice. A greater decrease in the levels of *Cxcl10* and *Nos2* transcripts and a higher increase in the levels of *Chil3* transcripts were detected in treated *Rab27a*$^{-/-}$ mice as compared with in nontreated *Rab27a*$^{-/-}$ mice (supplemental Figure 2B).

Ruxolitinib does not increase viral titers in cytotoxicity-impaired mice

In view of the genetic defect in cytotoxicity, LCMV persisted in both treated and nontreated *Prf1*$^{-/-}$ mice. In contrast, control mice eliminated LCMV by day 10 postinfection. The improvements in survival, clinical parameters, and recovery of tissue homeostasis observed in ruxolitinib-treated *Prf1*$^{-/-}$ mice were thus not related to efficient viral control, as was previously observed for anti-IFN-γ antibody therapy.[39] Importantly, there were no harmful consequences of ruxolitinib treatment on the viral load, as the latter remained stable up to 28 days postinfection (Figure 7A). The same was true in the *Rab27a*$^{-/-}$ murine model (Figure 7B).

Discussion

The present study was designed to evaluate the therapeutic efficacy of ruxolitinib in 2 murine models of primary HLH, as preclinical models of human HLH. We found that 2 weeks of ruxolitinib treatment in HLH-prone mice, initiated at the time they expressed full-blown HLH, inhibited JAK1/2-STAT1 signaling in vivo, significantly increased the long-term survival rate of *Prf1*$^{-/-}$ mice and corrected the clinical, biological, and histological features of HLH in both mice models, including cell infiltration of the CNS, which could only be analyzed in the *Rab27a*$^{-/-}$ mouse. Furthermore, ruxolitinib therapy appeared to accelerate tissue repair. These data strongly support the use of JAK1/2 inhibitors as a targeted therapy for primary, and potentially secondary, HLH. The rationale for ruxolitinib treatment is based on pathophysiological findings, and the treatment's efficacy was demonstrated in 2 murine models of primary HLH.

It was recently reported that high-dose oral administration of ruxolitinib (90 mg/kg twice daily) prevented the development of HLH manifestations in 2 murine disease models, including the *Prf1*$^{-/-}$ mouse.[48] One important aspect of our study is the demonstration that oral administration of ruxolitinib not only prevented the manifestations of HLH but, above all, enabled recovery from existing HLH-related damage. Furthermore, we showed that these effects could be elicited with a clinically relevant dose of ruxolitinib. In the phase 1 and phase 2 clinical trials reported to date, twice-daily doses of 15 to 50 mg/m^2 in children and 25 mg in adults were well tolerated.[44,58,59] These values are equivalent to the twice-daily therapeutic oral dose of 1 mg/kg per mouse used in the present study. Our dose level was high enough to downregulate STAT1 activation in circulating MNCs, correct all the clinical and biological manifestations of HLH, and significantly improve *Prf1*$^{-/-}$ mice survival, although no pharmacological data were collected in the present study. Interestingly, the 2-week course of ruxolitinib administered in the present study appears to be at least as efficacious in regard to *Prf1*$^{-/-}$ mice survival as the INF-γ neutralization previously proposed as an alternative therapeutic approach in HLH.[39,40] Use of a JAK1/2 inhibitor may be advantageous, as the JAK1/2 signaling pathway is downstream of the receptors for IFN-γ and other inflammatory cytokines (such as IL-2 and IL-6) found at high serum concentrations in HLH. This may be particularly true in secondary forms of HLH, in which IFN-γ may not always be necessary the first driving cytokine of HLH. The bioavailability

of anti-INF-γ antibody and ruxolitinib may differ. Ruxolitinib is a small molecule and may diffuse more easily in enlarged organs such as liver and spleen or may better cross the blood–brain barrier as discussed later. In any case, the possibility of having 2 different compounds with more or less similar activity may allow us to overcome the occurrence of unexpected adverse events that can never be excluded for one of them. Importantly, ruxolitinib has already been shown to have a good tolerance profile to treat patients with myelofibrosis disorder.[43,44] JAK1/2 inhibition therapy may therefore be a promising, targeted approach for achieving remission from the systemic inflammatory syndrome that characterizes HLH.

Of the various HLH features corrected under inhibition of JAK1/2 by ruxolitinib, the reduction in lymphocytic infiltration of the CNS deserves to be highlighted. Indeed, CNS involvement is a major concern in HLH and has a significant effect on the patient's long-term outcome.[23-26] About a third of the children with HLH exhibit CNS symptoms, and half show a moderately elevated cell count in the cerebrospinal fluid, many with sequelae post-HSCT.[60] With a molecular mass of 404.36, ruxolitinib might not diffuse easily through the blood–brain barrier under normal circumstances. A putative HLH-associated increase in the barrier's permeability[61] may enable the drug to enter the CNS; however, this hypothesis requires further evaluation.

Prominent cell infiltration and tissue damage in the liver, as well as in other organs, are also characteristic features of HLH in both humans and murine models.[37-39] Our results show that liver macrophage turnover contributes to liver damage and then recovery. In *Prf1*$^{-/-}$ mice, macrophage recruitment coincided with the peak in HLH manifestations and death. This pattern is similar to that previously reported in the context of bacterial infections.[51] In control mice, macrophage recruitment is followed by a second step, during which alternative macrophages are recruited, expand, and become activated to contribute to tissue repair. Interestingly, a large number of alternative activated macrophages were detected in the liver of ruxolitinib-treated *Prf1*$^{-/-}$ mice, despite the persistence of LCMV. This phenomenon was associated with a gene expression profile characteristic of tissue repair.[62] In a model of reversible hepatic fibrosis, it has been shown that restorative macrophages capable of resolving liver fibrosis are derived from recruited inflammatory monocytes after a phenotypic switch mediated by the ingestion of cellular debris.[63] A direct contribution of ruxolitinib treatment to this process is strongly suggested by the more pronounced decrease in expression levels of inflammation markers (*Cxcl10* and *Nos2*) and a greater increase in recovery markers (*Chil3* and *Il10*) in treated *Rab27a*$^{-/-}$ mice than in nontreated animals.

Overall, this study sets out the rationale for the use of ruxolitinib as a potent, anti-inflammatory treatment of primary HLH. When administered alone or in combination with other drugs, ruxolitinib may induce remission with potentially limited toxicity, at least when compared with conventional therapies such as etoposide and anti-T cell antibodies.[27,28] This may provide an additional benefit for the outcome of HSCT by reducing inflammation-related secondary complications, such as veno-occlusive disease or pulmonary arterial hypertension.[64,65] Further work will be aimed at precisely determining the pharmacological parameters of ruxolitinib administration in this context. Future studies will be nevertheless based on the data obtained in patients treated for other conditions, which suggests ruxolitinib could be used to treat HLH safely in humans.

Acknowledgments

The authors thank Bénédicte Neven for sharing ruxolitinib component and advice; Corina Dragu, Elena Marot, Cedrick Pauchard, and Imagine Institute's animal facility for their assistance; and Sophie Berissi from the histology department for technical support.

This work was supported by the French National Institutes of Health and Medical Research, the Agence Nationale de la Recherche (ANR HLH-Cytotox/ANR-12-BSV1-0020-01), the European Research Council (PIDImmun, advanced grant 249816), and the Imagine Foundation. S.M. was supported by fellowships from the Association pour la Recherche sur le Cancer and the Imagine Foundation. F.E.S. was supported by fellowships from the Association pour la Recherche sur le Cancer, the Agence Nationale de la Recherche, and Becas Chile.

Authorship

Contribution: S.M. designed, conducted, and analyzed experiments; A.G. performed and analyzed experiments; F.E.S. and A.F. discussed data; S.M., A.F., and G.d.S.B. wrote the manuscript; and S.M. and G.d.S.B. designed and supervised the overall research.

Conflict-of-interest disclosure: The authors declare no competing financial interests.

Correspondence: Geneviève de Saint Basile, Inserm U1163, Imagine Institute, Hôpital Necker-Enfants Malades, F-75015 Paris, France; e-mail: genevieve.de-saint-basile@inserm.fr.

References

1. de Saint Basile G, Ménasché G, Fischer A. Molecular mechanisms of biogenesis and exocytosis of cytotoxic granules. *Nat Rev Immunol.* 2010;10(8):568-579.
2. Filipovich AH. Hemophagocytic lymphohistiocytosis and other hemophagocytic disorders. *Immunol Allergy Clin North Am.* 2008;28(2):293-313.
3. Janka GE. Familial and acquired hemophagocytic lymphohistiocytosis. *Eur J Pediatr.* 2007;166(2): 95-109.
4. Janka GE. Familial and acquired hemophagocytic lymphohistiocytosis. *Annu Rev Med.* 2012;63: 233-246.
5. Janka GE, Lehmberg K. Hemophagocytic syndromes–an update. *Blood Rev.* 2014; 28(4):135-142.
6. Stepp SE, Dufourcq-Lagelouse R, Le Deist F, et al. Perforin gene defects in familial hemophagocytic lymphohistiocytosis. *Science.* 1999;286(5446): 1957-1959.
7. Feldmann J, Callebaut I, Raposo G, et al. Munc13-4 is essential for cytolytic granules fusion and is mutated in a form of familial hemophagocytic lymphohistiocytosis (FHL3). *Cell.* 2003;115(4):461-473.
8. zur Stadt U, Schmidt S, Kasper B, et al. Linkage of familial hemophagocytic lymphohistiocytosis (FHL) type-4 to chromosome 6q24 and identification of mutations in syntaxin 11. *Hum Mol Genet.* 2005;14(6):827-834.
9. Côte M, Ménager MM, Burgess A, et al. Munc18-2 deficiency causes familial hemophagocytic lymphohistiocytosis type 5 and impairs cytotoxic granule exocytosis in patient NK cells. *J Clin Invest.* 2009;119(12):3765-3773.
10. zur Stadt U, Rohr J, Seifert W, et al. Familial hemophagocytic lymphohistiocytosis type 5 (FHL-5) is caused by mutations in Munc18-2 and impaired binding to syntaxin 11. *Am J Hum Genet.* 2009;85(4):482-492.
11. Ménasché G, Pastural E, Feldmann J, et al. Mutations in RAB27A cause Griscelli syndrome associated with haemophagocytic syndrome. *Nat Genet.* 2000;25(2):173-176.
12. Nagle DL, Karim MA, Woolf EA, et al. Identification and mutation analysis of the complete gene for Chediak-Higashi syndrome. *Nat Genet.* 1996;14(3):307-311.
13. Barbosa MD, Nguyen QA, Tchernev VT, et al. Identification of the homologous beige and Chediak-Higashi syndrome genes. *Nature.* 1996;382(6588):262-265.
14. Tangye SG. XLP: clinical features and molecular etiology due to mutations in SH2D1A encoding SAP. *J Clin Immunol.* 2014;34(7):772-779.

15. Voskoboinik I, Smyth MJ, Trapani JA. Perforin-mediated target-cell death and immune homeostasis. *Nat Rev Immunol.* 2006;6(12):940-952.
16. Terrell CE, Jordan MB. Perforin deficiency impairs a critical immunoregulatory loop involving murine CD8(+) T cells and dendritic cells. *Blood.* 2013; 121(26):5184-5191.
17. Sepulveda FE, Maschalidi S, Vosshenrich CA, et al. A novel immunoregulatory role for NK-cell cytotoxicity in protection from HLH-like immunopathology in mice. *Blood.* 2015;125(9):1427-1434.
18. Jenkins MR, Rudd-Schmidt JA, Lopez JA, et al. Failed CTL/NK cell killing and cytokine hypersecretion are directly linked through prolonged synapse time. *J Exp Med.* 2015;212(3): 307-317.
19. Nagafuji K, Nonami A, Kumano T, et al. Perforin gene mutations in adult-onset hemophagocytic lymphohistiocytosis. *Haematologica.* 2007;92(7): 978-981.
20. Zhang K, Jordan MB, Marsh RA, et al. Hypomorphic mutations in PRF1, MUNC13-4, and STXBP2 are associated with adult-onset familial HLH. *Blood.* 2011;118(22):5794-5798.
21. Emmenegger U, Schaer DJ, Larroche C, Neftel KA. Haemophagocytic syndromes in adults: current concepts and challenges ahead. *Swiss Med Wkly.* 2005;135(21-22):299-314.
22. Hsieh SM, Chang SC. Insufficient perforin expression in CD8+ T cells in response to hemagglutinin from avian influenza (H5N1) virus. *J Immunol.* 2006;176(8):4530-4533.
23. Haddad E, Sulis ML, Jabado N, Blanche S, Fischer A, Tardieu M. Frequency and severity of central nervous system lesions in hemophagocytic lymphohistiocytosis. *Blood.* 1997;89(3):794-800.
24. Deiva K, Mahlaoui N, Beaudonnet F, et al. CNS involvement at the onset of primary hemophagocytic lymphohistiocytosis. *Neurology.* 2012;78(15):1150-1156.
25. Horne A, Trottestam H, Aricò M, et al; Histiocyte Society. Frequency and spectrum of central nervous system involvement in 193 children with haemophagocytic lymphohistiocytosis. *Br J Haematol.* 2008;140(3):327-335.
26. Henter JI, Nennesmo I. Neuropathologic findings and neurologic symptoms in twenty-three children with hemophagocytic lymphohistiocytosis. *J Pediatr.* 1997;130(3):358-365.
27. Henter JI, Aricò M, Egeler RM, et al. HLH-94: a treatment protocol for hemophagocytic lymphohistiocytosis. HLH study Group of the Histiocyte Society. *Med Pediatr Oncol.* 1997; 28(5):342-347.
28. Mahlaoui N, Ouachée-Chardin M, de Saint Basile G, et al. Immunotherapy of familial hemophagocytic lymphohistiocytosis with antithymocyte globulins: a single-center retrospective report of 38 patients. *Pediatrics.* 2007;120(3):e622-e628.
29. Henter JI, Horne A, Aricó M, et al. HLH-2004: Diagnostic and therapeutic guidelines for hemophagocytic lymphohistiocytosis. *Pediatr Blood Cancer.* 2007;48(2):124-131.
30. Jordan MB, Filipovich AH. Hematopoietic cell transplantation for hemophagocytic lymphohistiocytosis: a journey of a thousand miles begins with a single (big) step. *Bone Marrow Transplant.* 2008;42(7):433-437.
31. Fischer A, Cerf-Bensussan N, Blanche S, et al. Allogeneic bone marrow transplantation for erythrophagocytic lymphohistiocytosis. *J Pediatr.* 1986;108(2):267-270.
32. Jordan MB, Allen CE, Weitzman S, Filipovich AH, McClain KL. How I treat hemophagocytic lymphohistiocytosis. *Blood.* 2011;118(15): 4041-4052.
33. Henter JI, Elinder G, Söder O, Hansson M, Andersson B, Andersson U. Hypercytokinemia in familial hemophagocytic lymphohistiocytosis. *Blood.* 1991;78(11):2918-2922.
34. Mazodier K, Marin V, Novick D, et al. Severe imbalance of IL-18/IL-18BP in patients with secondary hemophagocytic syndrome. *Blood.* 2005;106(10):3483-3489.
35. Osugi Y, Hara J, Tagawa S, et al. Cytokine production regulating Th1 and Th2 cytokines in hemophagocytic lymphohistiocytosis. *Blood.* 1997;89(11):4100-4103.
36. Takada H, Takahata Y, Nomura A, Ohga S, Mizuno Y, Hara T. Increased serum levels of interferon-gamma-inducible protein 10 and monokine induced by gamma interferon in patients with haemophagocytic lymphohistiocytosis. *Clin Exp Immunol.* 2003;133(3):448-453.
37. Billiau AD, Roskams T, Van Damme-Lombaerts R, Matthys P, Wouters C. Macrophage activation syndrome: characteristic findings on liver biopsy illustrating the key role of activated, IFN-gamma-producing lymphocytes and IL-6- and TNF-alpha-producing macrophages. *Blood.* 2005;105(4): 1648-1651.
38. Jordan MB, Hildeman D, Kappler J, Marrack P. An animal model of hemophagocytic lymphohistiocytosis (HLH): CD8+ T cells and interferon gamma are essential for the disorder. *Blood.* 2004;104(3):735-743.
39. Pachlopnik Schmid J, Ho CH, Chrétien F, et al. Neutralization of IFNgamma defeats haemophagocytosis in LCMV-infected perforin- and Rab27a-deficient mice. *EMBO Mol Med.* 2009;1(2):112-124.
40. Jordan M, Locatelli F, Allen C, et al. A novel targeted approach to the treatment of hemophagocytic lymphohistiocytosis (HLH) with an anti-interferon gamma (IFNγ) monoclonal antibody (mAb), NI-0501: first results from a pilot phase 2 study in children with primary HLH [abstract]. Presented at: 57th American Society of Hematology meeting. December 8, 2015. Orlando, FL. LBA-3.
41. Xing L, Dai Z, Jabbari A, et al. Alopecia areata is driven by cytotoxic T lymphocytes and is reversed by JAK inhibition. *Nat Med.* 2014;20(9): 1043-1049.
42. Punwani N, Scherle P, Flores R, et al. Preliminary clinical activity of a topical JAK1/2 inhibitor in the treatment of psoriasis. *J Am Acad Dermatol.* 2012;67(4):658-664.
43. Harrison C, Kiladjian JJ, Al-Ali HK, et al. JAK inhibition with ruxolitinib versus best available therapy for myelofibrosis. *N Engl J Med.* 2012; 366(9):787-798.
44. Verstovsek S, Kantarjian H, Mesa RA, et al. Safety and efficacy of INCB018424, a JAK1 and JAK2 inhibitor, in myelofibrosis. *N Engl J Med.* 2010;363(12):1117-1127.
45. Quintás-Cardama A, Vaddi K, Liu P, et al. Preclinical characterization of the selective JAK1/2 inhibitor INCB018424: therapeutic implications for the treatment of myeloproliferative neoplasms. *Blood.* 2010;115(15):3109-3117.
46. O'Shea JJ, Plenge R. JAK and STAT signaling molecules in immunoregulation and immune-mediated disease. *Immunity.* 2012;36(4):542-550.
47. Yarilina A, Xu K, Chan C, Ivashkiv LB. Regulation of inflammatory responses in tumor necrosis factor-activated and rheumatoid arthritis synovial macrophages by JAK inhibitors. *Arthritis Rheum.* 2012;64(12):3856-3866.
48. Das R, Guan P, Sprague L, et al. Janus kinase inhibition lessens inflammation and ameliorates disease in murine models of hemophagocytic lymphohistiocytosis. *Blood.* 2016;127(13): 1666-1675.
49. Spoerl S, Mathew NR, Bscheider M, et al. Activity of therapeutic JAK 1/2 blockade in graft-versus-host disease. *Blood.* 2014;123(24):3832-3842.
50. Sepulveda FE, Debeurme F, Ménasché G, et al. Distinct severity of HLH in both human and murine mutants with complete loss of cytotoxic effector PRF1, RAB27A, and STX11. *Blood.* 2013;121(4): 595-603.
51. Blériot C, Dupuis T, Jouvion G, Eberl G, Disson O, Lecuit M. Liver-resident macrophage necroptosis orchestrates type 1 microbicidal inflammation and type-2-mediated tissue repair during bacterial infection. *Immunity.* 2015;42(1):145-158.
52. Olin RL, Nichols KE, Naghashpour M, et al. Successful use of the anti-CD25 antibody daclizumab in an adult patient with hemophagocytic lymphohistiocytosis. *Am J Hematol.* 2008;83(9):747-749.
53. Mantovani A, Biswas SK, Galdiero MR, Sica A, Locati M. Macrophage plasticity and polarization in tissue repair and remodelling. *J Pathol.* 2013; 229(2):176-185.
54. Murray PJ, Wynn TA. Protective and pathogenic functions of macrophage subsets. *Nat Rev Immunol.* 2011;11(11):723-737.
55. MacMicking J, Xie QW, Nathan C. Nitric oxide and macrophage function. *Annu Rev Immunol.* 1997; 15:323-350.
56. Raes G, De Baetselier P, Noël W, Beschin A, Brombacher F, Hassanzadeh Gh G. Differential expression of FIZZ1 and Ym1 in alternatively versus classically activated macrophages. *J Leukoc Biol.* 2002;71(4):597-602.
57. Colegio OR, Chu NQ, Szabo AL, et al. Functional polarization of tumour-associated macrophages by tumour-derived lactic acid. *Nature.* 2014; 513(7519):559-563.
58. Loh ML, Tasian SK, Rabin KR, et al. A phase 1 dosing study of ruxolitinib in children with relapsed or refractory solid tumors, leukemias, or myeloproliferative neoplasms: A Children's Oncology Group phase 1 consortium study (ADVL1011). *Pediatr Blood Cancer.* 2015;62(10):1717-1724.
59. Eghtedar A, Verstovsek S, Estrov Z, et al. Phase 2 study of the JAK kinase inhibitor ruxolitinib in patients with refractory leukemias, including postmyeloproliferative neoplasm acute myeloid leukemia. *Blood.* 2012;119(20):4614-4618.
60. Trottestam H, Horne A, Aricò M, et al; Histiocyte Society. Chemoimmunotherapy for hemophagocytic lymphohistiocytosis: long-term results of the HLH-94 treatment protocol. *Blood.* 2011;118(17):4577-4584.
61. Abbott NJ. Inflammatory mediators and modulation of blood-brain barrier permeability. *Cell Mol Neurobiol.* 2000;20(2):131-147.
62. Martinez FO, Gordon S. The M1 and M2 paradigm of macrophage activation: time for reassessment. *F1000Prime Rep.* 2014;6:13.
63. Ramachandran P, Pellicoro A, Vernon MA, et al. Differential Ly-6C expression identifies the recruited macrophage phenotype, which orchestrates the regression of murine liver fibrosis. *Proc Natl Acad Sci USA.* 2012;109(46): E3186-E3195.
64. Ouachée-Chardin M, Elie C, de Saint Basile G, et al. Hematopoietic stem cell transplantation in hemophagocytic lymphohistiocytosis: a single-center report of 48 patients. *Pediatrics.* 2006; 117(4):e743-e750.
65. Jodele S, Hirsch R, Laskin B, Davies S, Witte D, Chima R. Pulmonary arterial hypertension in pediatric patients with hematopoietic stem cell transplant-associated thrombotic microangiopathy. *Biol Blood Marrow Transplant.* 2013;19(2): 202-207.